Synthesis, characterization and investigation of molecular motion by variable temperature ^{1}H NMR of the bis(quadridentate)zirconium(IV) complexes bis(*N,N'*-disalicylidene-*cis*-1,2-diaminocyclohexanato)zirconium(IV) and bis(*N,N'*-disalicylidene-*trans*-1,2-diaminocyclohexanato)zirconium(IV), and comparisons with bis(*N,N'*-disalicylidene-1,2-phenylenediaminato)zirconium(IV). Crystal and molecular structure of the racemic Zr(*trans*-dsd)$_2$ and Zr(*S,S-trans*-dsd)$_2$ complexes*

Marvin L. Illingsworth**, Brian P. Cleary†, Andrew J. Jensen††, Leslie J. Schwartz***
Department of Chemistry, Rochester Institute of Technology, Rochester, NY 14623 (USA)

and Arnold L. Rheingold†††
Department of Chemistry and Biochemistry, University of Delaware, Newark, DE 19716 (USA)

(Received September 14, 1992; revised December 18, 1992)

Abstract

Variable temperature ^{1}H NMR over the range from 165.9 to 19.9 °C in d^6-dimethyl sulfoxide and 22.1 to −95.4 °C in d^2-methylene chloride is employed to investigate the molecular motions in the eight-coordinate zirconium complexes bis(*N,N'*-disalicylidene-*cis*-1,2-diaminocyclohexanato)zirconium(IV), Zr(*cis*-dsd)$_2$; bis(*N,N'*-disalicylidene-*trans*-1,2-diaminocyclohexanato)zirconium(IV), Zr(*trans*-dsd)$_2$; and bis(*N,N'*-disalicylidene-1,2-phenylenediaminato)zirconium(IV), Zr(dsp)$_2$. For Zr(*cis*-dsd)$_2$, the resolution of one methine signal into separate axial (upfield) and equatorial (downfield) signals at low temperature is consistent with the chair-to-chair interconversion of the fused cyclohexane ring becoming slow on the NMR time scale. A coalescence temperature of *c.* −47 °C and a thermodynamic barrier of $\Delta G^{\ddagger}(298) = 46.5 \pm 0.9$ kJ mol^{-1}, $\Delta H^{\ddagger} = 27 \pm 3$ kJ mol^{-1} and $\Delta S^{\ddagger} = -66 \pm 13$ J mol^{-1} K^{-1} are obtained for this process. The resolution of six imine signals at −95.4 °C from two ambient temperature imine signals is attributed to slow interconversion of isomers which arise from different ligand wrapping geometries, cyclohexane ring conformations, and/or polytopal coordination geometries. For Zr(*trans*-dsd)$_2$, the resolution of a second set of salicylidene NMR signals as the temperature is decreased is likewise attributed to the slow interconversion of isomers. However, since only one set of averaged signals is observed at high temperature, these isomers must possess symmetrical salicylidene moieties. For Zr(dsp)$_2$, comparable changes were not observed over the temperature range studied, despite the fact that both dsp(2−) and dsd(2−) ligands are capable of considerable non-planarity. The two new zirconium complexes, Zr(*cis*-dsd)$_2$ and Zr(*trans*-dsd)$_2$, are synthesized from Zr(O-n-C$_4$H$_9$)$_4$ butanol solvate and Schiff bases made from *cis*- and *trans*-diaminocyclohexane (DACH), and characterized by elemental analysis, IR, UV–Vis, ^{1}H and ^{13}C NMR (the latter able to distinguish Zr(*R,R-trans*-dsd)(*S,S-trans*-dsd) from other Zr(*trans*-dsd)$_2$ isomers), thermogravimetric analysis, optical rotation for the separate enantiomers Zr(*R,R-trans*-dsd)$_2$ and Zr(*S,S-trans*-dsd)$_2$, and single crystal X-ray diffraction analysis for Zr(*trans*-dsd)$_2$. Hitherto unpublished ^{13}C NMR results for Zr(dsp)$_2$ are included in order to facilitate making assignments. Details of the crystallography include: formula $C_{40}H_{40}N_4O_4Zr$, space group *Fddd* with $a = 15.232(3)$, $b = 16.994(4)$, $c = 26.711(5)$ Å, $V = 6914(2)$ Å^3, $Z = 8$, and $D_{calc} = 1.406$ g cm^{-3}; refinement of 152 variables using 2283 reflections collected (1820 independent and observed) converge at $R = 3.84\%$. Details of the crystallography for the Zr(*S,S-trans*-dsd)$_2$ isomer, space group $P\bar{1}$, can be obtained. Testing of the new complexes for anticancer activity was performed by Bristol-Myers and was negative.

*This paper was presented in part at the 29th International Coordination Chemistry Conference in Lausanne, Switzerland, July 20–24, 1992.

**Author to whom general correspondence should be addressed.

†Present address: Chemistry Department, University of Rochester, Rochester, NY 14627, USA.

††Present address: Fisons Corporation, 331 Clay Rd., Rochester, NY 14623, USA.

***On leave from St. John Fisher College. Author to whom computer simulation inquiries should be addressed: Department of Chemistry, St. John Fisher College, Rochester, NY 14618, USA.

†††Author to whom crystallographic inquiries should be addressed.

0020-1693/93/$6.00

Introduction

Further study of eight-coordinate complexes is merited, in part, because of their potential application as components of coordination polymers [1] and their use in ligand exchange studies. The same is true for complexes of diaminocyclohexane (DACH) and its derivatives, due in part to the excellent anticancer activity displayed by their platinum complexes [2], which are known to retain their activity even longer than cisplatin, and, furthermore, due to the stereoselectivity displayed by complexes having quadridentate DACH Schiff base ligands [3] and the chiral recognition displayed by complexes having either DACH derivatives or DACH itself as ligands [2a, 3f, 4]. The interconversion of various isomers is an important feature in many of these systems.

Variable temperature NMR (VT-NMR) has become a standard method of obtaining thermodynamic values which reflect the energy barriers that exist for specific molecular motions [5]. The technique has been used to investigate A and B dodecahedral site exchange [5a], chelate ring conformational interconversion [5a], and polytopal rearrangement [6] of isomers in eight-coordinate complexes, and it has also been extensively used to study complexes of *cis*-diaminocyclohexane (*cis*-DACH) [2b, 7] and its derivatives [8], where $\lambda \rightleftharpoons \delta$ interconversion of the chelate ring accompanies interconversion of the fused cyclohexane ring. Complexes of *trans*-DACH, however, which exist as *R,R*- and *S,S*-enantiomeric forms, are not so often studied in this manner [9] since equatorial nitrogen atoms reportedly stabilize the chelate ring much more than axial nitrogens [2b, 3d, 4a, 10].

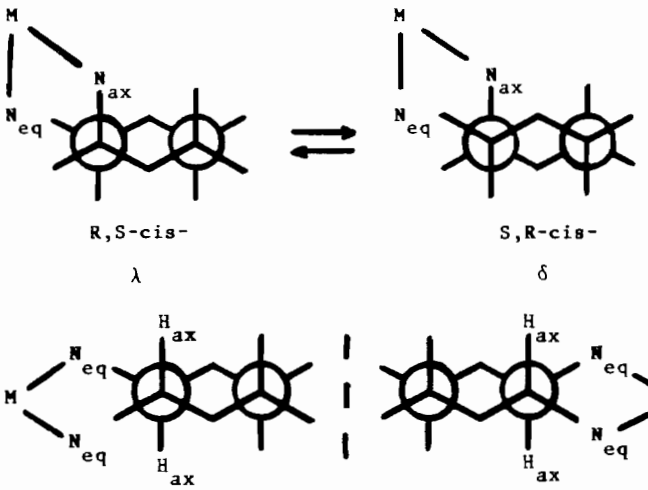

Therefore, we wish to report herein the results of a variable temperature ^{1}H NMR study of two new eight-coordinate zirconium complexes which contain *cis*- and *trans*-DACH components, bis(*N,N'*-disalicylidene-*cis*-1,2-diaminocyclohexanato)zirconium(IV), Zr(*cis*-dsd)$_2$, and bis(*N,N'*-disalicylidene-*trans*-1,2-diaminocyclohexanato)zirconium(IV), Zr(*trans*-dsd)$_2$. VT-NMR results for the previously reported complex bis(*N,N'*-disalicylidene-1,2-phenylenediaminato)zirconium(IV)[11], Zr(dsp)$_2$, which likewise is eight-coordinate but which lacks cyclohexane rings, are presented for comparison purposes.

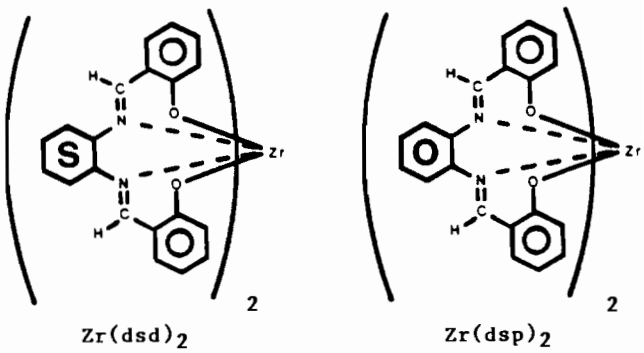

The new complexes have been characterized using elemental analyses, IR, UV–Vis, ^{1}H and ^{13}C NMR, thermogravimetric analysis, optical rotation for Zr(*R,R-trans*-dsd)$_2$ and Zr(*S,S-trans*-dsd)$_2$, and single crystal X-ray diffraction analysis for racemic Zr(*trans*-dsd)$_2$ and Zr(*S,S-trans*-dsd)$_2$. Hitherto unpublished ^{13}C NMR results for Zr(dsp)$_2$ are included to facilitate making assignments.

In 'Discussion', thermodynamic parameters and rate constants for the cyclohexane ring interconversion in Zr(*cis*-dsd)$_2$ obtained from the VT-NMR experiments are compared to those for other structurally related compounds. Also, the role of the cyclohexane and salicylidene substituents in the stabilization of different isomers, and in the interconversion of these isomers, is considered.

Experimental

Reagent grade solvents and chemicals were used. Salicylaldehyde (Aldrich) was purified by reduced pressure distillation. The other reagents, *cis*-1,2-diaminocyclohexane, (±)-*trans*-1,2-diaminocyclohexane, 1*R*,2*R*-(−)-1,2-diaminocyclohexane, (1*S*,2*S*)-(+)-1,2-diaminocyclohexane (Aldrich) and tetra-n-butoxyzirconium(IV) butanol solvate ($Zr(O\text{-}n\text{-}Bu)_4 \cdot n\text{-}BuOH$, Alfa) were used without further purification.

The bis(*N*,*N'*-disalicylidene-1,2-phenylenediaminato)zirconium(IV), $Zr(dsp)_2$, was prepared as previously described [11]. Its identity and purity were confirmed by decomposition point, thin layer chromatography, and ^1H NMR.

The dinitrogen gas (Air Products) used in the complexation reactions was dried over calcium hydride (Aldrich). All thin layer chromatograms were obtained on silica (Kodak).

N,N'-Disalicylidene-cis-1,2-diaminocyclohexane, cis-H_2dsd

To a solution of 7.48 ml (70.3 mmol) of freshly distilled salicylaldehyde in 100 ml of absolute ethanol were added 4.00 g (35.1 mmol) of *cis*-1,2-diaminocyclohexane and a stirbar. The reaction was stirred and maintained at reflux for 24 h. Upon cooling and suction filtering, a yield of 10.65 g (94.2%) of a fluffy yellow solid was obtained, m.p. 141–142 °C. One spot was observed on the thin layer chromatogram ($R_f = 0.5$,with eluent 1:1 chloroform:cyclohexane).

Prior to elemental analysis the ligand was dried under vacuum (*c.* 25 mm Hg) at 100 °C for 3 days to remove any remaining solvent. *Anal.* Calc. for $C_{20}H_{22}N_2O_2$: C, 74.51; H, 6.88; N, 8.69. Found: C, 74.38; H, 6.87; N, 8.73%.

Bis(N,N'-disalicylidene-cis-1,2-diaminocyclohexanato)-zirconium(IV), Zr(cis-dsd)$_2$

Under a dry dinitrogen atmosphere (glovebag), a stirbar and 4.66 ml (10.8 mmol) of $Zr(O\text{-}n\text{-}Bu)_4 \cdot n\text{-}BuOH$ were added to a solution of 7.00 g (21.7 mmol) of *cis*-H_2dsd in 250 ml of absolute ethanol. The reaction mixture was stoppered, removed from the glovebag and fitted with a condenser equipped with a drying tube ($CaCl_2$). The reaction mixture was stirred and maintained at reflux for 20 h. After the suspension was cooled, a yield of 7.60 g (96.3%) of a cream–white colored solid was isolated by suction filtration. The product discolored between 280 and 366 °C, and exhibited one spot on the thin layer chromatogram ($R_f = 0.4$, with eluent 1:1 chloroform:cyclohexane).

Prior to elemental analysis the complex was dried under vacuum (*c.* 25 mm Hg) at 100 °C for 3 days. *Anal.* Calc. for $C_{40}H_{40}N_4O_4Zr$: C, 65.54; H, 5.50; N, 7.64; Zr, 12.4. Found: C, 65.50; H, 5.47; N, 7.62: Zr, 12.2%.

(±)-N,N'-Disalicylidene-trans-1,2-diaminocyclohexane, (±)-trans-H_2dsd

To a solution of 23.0 ml (216 mmol) of freshly distilled salicylaldehyde in 500 ml of absolute ethanol were added 13.1 ml (108 mmol) of (±)-*trans*-1,2-diaminocyclohexane and a stirbar. The reaction was stirred and maintained at reflux for 12 h. Upon cooling, a yellow precipitate formed. A yield of 28.2 g (81.%) of a fluffy yellow solid was isolated by suction filtration, m.p. 119–119.5 °C (lit. 119 °C [12]). The ligand exhibited one spot on the thin layer chromatogram ($R_f = 0.85$, eluent 10:0.5 chloroform:cyclohexane).

(±)-Bis(N,N'-disalicylidene-trans-1,2-diaminocyclohexanato)zirconium(IV), Zr(trans-dsd)$_2$

Under a dry dinitrogen atmosphere (glovebag), a stirbar and 6.46 ml (15.0 mmol) of $Zr(O\text{-}n\text{-}Bu)_4 \cdot n\text{-}BuOH$ were added to a solution of 9.66 g (30.0 mmol) of (±)-*trans*-H_2dsd in 500 ml of absolute ethanol. The reaction mixture was stoppered, removed from the glovebag and fitted with a condenser equipped with a drying tube ($CaCl_2$). The reaction mixture was stirred and maintained at reflux for 18.5 h. The suspension was then cooled and suction filtered, yielding 9.96 g (90.8%) of a light yellow solid. The product discolored between 280 and 390 °C and exhibited one spot on the thin layer chromatogram ($R_f = 0.5$, with eluent 1:1 chloroform:cyclohexane).

Prior to elemental analysis the complex was dried at 100 °C under vacuum (*c.* 25 mm Hg) for 3 days to remove any solvent. *Anal.* Calc. for $C_{40}H_{40}N_4O_4Zr$: C, 65.54; H, 5.50; N, 7.64; Zr, 12.4. Found: C, 65.56; H, 5.53; N, 7.55; Zr, 12.1%.

(+)-Bis(N,N'-disalicylidene-R,R-trans-1,2-diaminocyclohexanato)zirconium(IV), Zr(R,R-trans-dsd)$_2$ and (−)-bis(N,N'-disalicylidene-S,S-trans-1,2-diaminocyclohexanato)zirconium(IV), Zr(S,S-trans-dsd)$_2$

The resolved Schiff base ligands were prepared in the above manner from the resolved diaminocyclohexanes, but failed to crystallize upon cooling. The solvent was therefore removed, and the resulting oils used in complexation reactions also as described above. The thin layer chromatograms each showed one spot.

For $Zr(R,R\text{-trans-dsd})_2$, an overall yield of 88.2% was obtained. *Anal.* Calc. for $C_{40}H_{40}N_4O_4Zr$: C, 65.54; H, 5.50; N, 7.64; Zr, 12.4. Found: C, 65.81; H, 5.54; N, 7.68; Zr, 12.3%. $[\alpha] = +52.79$.

For $Zr(S,S\text{-trans-dsd})_2$, an overall yield of 77.2% was obtained. *Anal.* Calc. for $C_{40}H_{40}N_4O_4Zr$: C, 65.54; H, 5.50; N, 7.64; Zr, 12.4. Found: C, 65.80; H, 5.53; N, 7.65; Zr, 12.4%. $[\alpha] = -57.13$.

Characterization

All IR spectra were obtained as KBr mulls using a Perkin-Elmer model 681 grating spectrophotometer and calibrated against polystyrene. The ambient temperature ^{1}H NMR spectra of *cis*-H_2dsd, *trans*-H_2dsd, H_2dsp, Zr(*cis*-dsd)$_2$, Zr(*trans*-dsd)$_2$, Zr(*R,R-trans*-dsd)$_2$, Zr(*S,S-trans*-dsd)$_2$ and Zr(dsp)$_2$ dissolved in $CDCl_3$ with TMS as the internal reference were obtained using a Nicolet NT-200 NMR spectrometer at 200 MHz. The ambient temperature proton decoupled ^{13}C NMR spectra of each of these samples were also obtained in $CDCl_3$ with TMS using a Bruker WP200 SY at 50.33 MHz. UV–Vis spectra were obtained as methylene chloride solutions using a Perkin-Elmer 552A UV–Vis spectrophotometer. The optical rotations for Zr(*R,R-trans*-dsd)$_2$ and Zr(*S,S-trans*-dsd)$_2$ were determined on a Perkin-Elmer model 241 polarimeter using the 589 nm Na line in methylene chloride at 23.0 °C, at *c*. 1 g/100 ml, and were corrected for exact concentration. Thermal gravimetric analyses were obtained using a Perkin-Elmer TGS-2 thermogravimetric analyzer, a Perkin-Elmer System 4 thermal analysis microprocessor controller, a Perkin-Elmer heater controller, a Perkin-Elmer gas selector, a Perkin-Elmer TGS-2 balance controller, and a Perkin-Elmer data thermal analysis station. Thermal plots were obtained using a Perkin-Elmer Graphics Plotter 2. The temperature range investigated was 30–500 °C, with a heating rate of 10.00° min^{-1}. Corrected thermogravimetric analysis temperatures were obtained using a temperature calibration curve. Uncorrected melting points were determined in a Laboratory Devices MEL-TEMP melting point apparatus. Elemental analyses for carbon, hydrogen and nitrogen were performed at Microlytics (P.O. Box 199, South Deerfield, MA 01373). Zirconium analysis was performed gravimetrically (as ZrO_2) at the Rochester Institute of Technology.

X-ray data collection and refinement

Crystal data are presented in Table 1. X-ray data were collected using a Nicolet R3m/μ, in the 2θ range of 4–50° using modified ω scans. Of 2283 reflections collected ($h = \pm 21$, $k = +23$, $l = +36$) for a colorless blocked crystal (0.27 × 0.32 × 0.31 mm), 1820 were independent and observed ($F_o > 5\sigma(F_o)$). Lattice parameters were obtained from the least-squares fit of 25 reflections, $20 \leqslant 2\theta \leqslant 25°$. The structure was solved by direct methods, and refined by full-matrix least-squares refinement on 152 parameters with all non-hydrogen atoms anisotropic. Hydrogen atoms were all located and isotropically refined. Atomic coordinates are provided in Table 2, and selected bond distances and angles in Table 3.

All computations used SHELXTL (5.1) software (G. Sheldrick, Nicolet (Siemens), Madison WI). For additional crystallographic data see 'Supplementary material'.

TABLE 1. Crystal and refinement data for Zr(*trans*-dsd)$_2$

Chemical formula	$C_{40}H_{40}N_4O_4Zr$
Formula weight	731.5
a (Å)	15.232(3)
b (Å)	16.994(4)
c (Å)	26.711(5)
V (Å^3)	6914(2)
T (K)	298
λ (Å)	0.71073
Space group	*Fddd*
Z	8
D_x (g cm^{-3})	1.406
R^a	0.0356
$R_w{}^b$	0.0384

$^aR = \Sigma(F_o - F_c)/\Sigma F_o$. $^bR_w = \{\Sigma w(F_o - F_c)^2/\Sigma w F_o^2\}^{1/2}$; $w^{-1} = \sigma^2(F_o) + gF_o^2$.

TABLE 2. Atomic coordinates (×10^4) and isotropic thermal parameters (Å^2 × 10^3)

	x	*y*	*z*	U^a
Zr	1250	1250	1250	28.8(1)
O(1)	779(1)	445(1)	1773(1)	43(1)
N(1)	2551(1)	650(1)	1606(1)	35(1)
C(1)	964(2)	−291(1)	1884(1)	39(1)
C(2)	283(2)	−840(2)	1968(1)	50(1)
C(3)	475(2)	−1610(2)	2102(1)	61(1)
C(4)	1340(2)	−1847(2)	2173(1)	66(1)
C(5)	2022(2)	−1320(1)	2091(1)	57(1)
C(6)	1849(2)	−544(1)	1932(1)	41(1)
C(7)	2580(1)	−21(1)	1828(1)	42(1)
C(8)	3378(1)	1094(1)	1521(1)	38(1)
C(9)	4223(2)	634(2)	1634(1)	51(1)
C(10)	5042(2)	1120(2)	1519(1)	65(1)

^{a}Equivalent isotropic *U* defined as one third of the trace of the orthogonalized U_{ij} tensor.

Variable temperature ^{1}H NMR

All non-ambient temperature ^{1}H NMR spectra were recorded on a Varian XL-400 NMR spectrometer at 400 MHz.

Low temperature ^{1}H NMR spectra of the complexes down to *c*. −95 °C were obtained individually as CD_2Cl_2 solutions with TMS as the internal reference. To determine if the complexes remained dissolved at −95.1 °C, they were separately dissolved in methylene chloride, placed into a methylene chloride slush bath prepared with liquid dinitrogen, and allowed to equilibrate for 5 min. The contents of the sample tubes were then checked for complex precipitation and solvent solidification, and neither was observed.

Elevated temperature ^{1}H NMR spectra of the free ligands, complexes, and mixtures of the ligands and complexes were obtained after temperature equilibra-

TABLE 3. Characterization data for the new zirconium complexes and their corresponding Schiff base ligands

H_2(*cis*-dsd)	Zr(*cis*-dsd)$_2$	H_2(*trans*-dsd)$_2$	Zr(*trans*-dsd)$_2$[a]	Assignment
Spectral data				
IR (cm^{-1})[b]				
3600		3600		
3400br, w	–	3300br, w	–	(H–O)ϕ
3080w	3070	3080	3080	
	3020w	3020w	3020w	H–C, aromatic
2950	2940	2960	2980	
2860m	2860m	2860m	2860m	H–C, aliphatic
1630s	1635s	1635s	1625s	imine
1580s	1550s	1585s	1555s	C=C, aromatic
1500s	1480s	1500s	1475s	C=C, aromatic
1280s	1325s	1280s	1325s	(ϕ-O)
UV–Vis (cm^{-1})[c]				
31500	29900	31800	29700	imine π–π^*
(3.99)	(4.25)	(4.04)	(4.23)	
38800	> 41000	39400	> 41000	aromatic ring
(4.42)	(–)	(4.43)	(–)	π–π^*
^1H *NMR* (δ)[d]				
13.43s(br)[e]	–[e]	13.00s(br)[e]	–[e]	H–O
8.54s (2)	8.41s (2)	8.46s (2)	8.30s[f] } (4)	imine
	8.33 s(2)		8.28s }	
7.40d (2)	7.28d (2)	7.34d (2)	7.22d[f] } (4)	aromatic
7.30t (2)	7.14m (4)	7.24t (2)	7.15d }	
6.85m (4)	6.96t (2)	6.82m (4)	7.02m (4)	
	6.52t (2)		6.44t[f] } (4)	
	6.41m (2)		6.40t }	
	6.24d (2)		6.27d[f] } (4)	
			6.23d }	
3.64m (2)	4.62d (4)[g]	3.58m (2)	4.23m (4)	H–C(N), chxn
1.72m (6)	2.68m (4)	1.85d (2)	~2.5[h]	H–C(C), chxn
	1.78m (8)	1.76d (2)	2.04m (4)	
1.52m (2)	1.65m (4)	1.59m (2)	1.69m (4)	
		1.41m (2)	1.58m (4)	
^{13}C *NMR* (δ)[i]				
	163.05			imine
164.03	162.92	164.68	162.86	*C*=N
161.24	161.59	161.01	158.48	aromatic
		160.98		C–O
132.10	133.19	132.06	133.38	aromatic
131.32	133.03	131.37	133.28	C=C
118.85	132.87	118.68	133.02	
118.32	122.12	118.46	122.30[j]	
116.94	121.77	116.74	118.86	
	118.62		115.45	
	118.49			
	115.63			
	115.45			
69.38	68.54	72.52	66.33[j]	chxn
	67.01			*C*–N
30.62	28.25	33.01	30.90[j]	chxn
	28.01			C–C
22.44	22.87	24.11	25.57[j]	
	22.30			

(continued)

Table 3. (*continued*)

Thermogravimetric analysis (°C)[k]		
340	365	Onset of weight loss (N_2)
380	385	Major feature (N_2)
470	475	Major feature (N_2)
350	380	Onset of weight loss (air)
365	395	Major feature (air)
420	425	Major feature (air)

[a]Racemic Zr(*trans*-dsd)$_2$ has the same spectral properties as Zr(*R,R-trans*-dsd)$_2$ and Zr(*S,S-trans*-dsd)$_2$ optical isomers. [b]Conditions: KBr mulls, polystyrene as external calibration; abbreviations: s = strong, m = medium, w = weak, br = broad. [c]All spectra obtained in methylene chloride; logarithms of the molar absorptivities are in parentheses. [d]All spectra are in DMSO-d^6, with Me_4Si as internal standard; the peak integration is given in parentheses; abbreviations: s = singlet, d = doublet, t = triplet, m = multiplet, br = broad. [e]Phenolic protons were observed in $CDCl_3$. [f]Observed in the Varian XL-400 spectra; the downfield signal is only *c.* 30% intensity of the upfield signal. [g]Appears as a broad singlet in CD_2Cl_2. [h]Under a DMSO signal; 2.51d (4) (0.005 ppm) in CD_2Cl_2. [i]All spectra are in $CDCl_3$, with the solvent peaks used as internal standard, and are proton decoupled. The proton decoupled ^{13}C NMR chemical shifts for H_2dsp and Zr(dsp)$_2$, which have not previously been reported, are respectively: 163.74, 161.35, 142.55, 133.29, 132.27, 127.58, 119.76, 119.22, 118.89, 117.51, and 164.96, 160.17, 146.33, 134.73, 133.89, 127.75, 122.60, 120.34, 118.59, 116.13. [j]Appear as double peaks due to Zr(*R,R-trans*-dsd)(*S,S-trans*-dsd). [k]A 30–500 °C temperature range was investigated with a heating rate of 10.00° min^{-1}; for the thermograms for Zr(*cis*-dsd)$_2$, in both dinitrogen and air atmospheres, see 'Supplementary material', Fig. 4s. Upon heating in air at *c.* 600 °C, each complex produces a white residue which is 16.7% by mass of the original sample, and thus is attributed to ZrO_2 (calc.: 16.8%).

tion at 165 °C (oil bath) for 1 h, as DMSO-d_6 solutions using the DMSO-d_6 solvent as the internal reference.

Conformation analyses

The methine region of the variable temperature NMR spectra of Zr(*cis*-dsd)$_2$ was simulated using a program [13] that calculates spectra for systems undergoing 2-site A⇌X exchange, where the A and X nuclei each experience coupling. The inputted parameters consist of the chemical shift difference in the absence of exchange, the exchange lifetime, a coupling constant (*CC*), and an inhomogeneous broadening value (*LB*). The last three parameters allow the following effects to be incorporated into the simulations as a function of increasing temperature: (1) the broadening, coalescence and sharpening of the methine signals, (2) the diminishing appearance of coupling between the two methine protons as they become more equivalent, (3) the averaging of the coupling of the methine protons to the β-protons, (4) the presence of inhomogeneous broadening, and (5) the splitting of the methine peaks due to the presence of the two different salicylidene moieties (*vide infra*). The exchange lifetime controls effect (1), *LB* incorporates effects (2)–(4), and *CC* models effect (5). [The magnitudes of the temperature-dependent couplings (2) and (3) are hypothesized to be comparable to that of the inhomogeneous broadening (4), and much smaller than the splitting due to the different salicylidene moieties (5) based on a comparison between the observed methine peak splitting in Zr(*trans*-dsd)$_2$ at −93.6 °C (*c.* 5 Hz) and in Zr(*cis*-dsd)$_2$ at −95.4 °C (*c.* 20 Hz). Since the spectra of the two complexes should have similar inhomogeneous broadening, and the couplings should be *larger* in the *trans* complex, the larger splitting in the *cis* complex is attributed to differences in the salicylidene moieties.]

For each experimental spectrum, LB and CC were varied between extreme values, thus giving a range of possible rate constants describing the cyclohexane ring interconversion and the simultaneous δ⇌λ interconversion of the fused five-membered chelate ring. *LB* was varied between 1 and 18 Hz, the extreme values obtained by simulating the lowest temperature spectrum in the limits where the linewidths are due either entirely to motional broadening or else entirely to inhomogeneous broadening, respectively. In the slow motional regime, a large inhomogeneous linewidth forces a small rate constant (and vice versa), while in the fast motional regime, a large inhomogeneous linewidth forces a large rate constant (and vice versa). *CC* was varied between values consistent with the observed peak splittings; these ranged from 1 to 35 Hz (the splitting is approximately 20 Hz in the lowest temperature spectrum). The −67.4 and −23.1 °C spectra, flanking the coalescence temperature (estimated to be −47 °C) are the most reliably simulated since they are almost independent of the values of *LB* and *CC*.

The chemical shift difference in the absence of exchange was taken to be 470 Hz, independent of temperature.

Results

Synthesis and characterization

The bis(quadridentate Schiff base)zirconium(IV) complexes, Zr(*cis*-dsd)$_2$, racemic Zr(*trans*-dsd)$_2$, Zr(*R,R*-

trans-dsd)$_2$ and Zr(*S,S-trans*-dsd)$_2$, have successfully been prepared from tetra(n-butoxy)zirconium(IV) n-butanol solvate and the appropriate premade Schiff base according to the reaction

$$Zr(O\text{-}n\text{-}Bu)_4 \cdot n\text{-}BuOH + 2H_2dsd \xrightarrow[(-5n\text{-}BuOH)]{\text{abs. EtOH, } \Delta} Zr(dsd)_2$$

Ambient temperature spectral data (IR, UV–Vis, ^{1}H and ^{13}C NMR), and thermal data for the new complexes (and free Schiff bases, where appropriate) are collected in Table 3.

The ORTEP plot and the atom numbering scheme for racemic Zr(*trans*-dsd)$_2$ are depicted in Figs. 1 and 2, respectively. Bond distances, bond angles and edge lengths for the coordination sphere are summarized in Tables 4 and 5. For deviations of the donor atoms from the least-squares mean trapezoidal planes, both with and without zirconium (which are all less than 0.05 Å, Table Is), and torsional angles in the coordinated Schiff base ligands (Table IIs) see 'Supplementary material'. As in Zr(dsp)$_2$ [11] and Zr(adsp)$_2$ [1a], the trapezoidal planes in Zr(*trans*-dsd)$_2$ are essentially perpendicular once again indicating a dodecahedral (pseudo D_{2d} or $42m$) coordination polyhedron. The dodecahedral geometry in this case, however, is perfectly regular, with all δ angles* [14] being identical (22.70°), and with $\theta_A = 35.2°$, $\theta_B = 69.9°$ and Zr–N(av.)/Zr–O(av.) = 1.16 [15]. The ligands once again span *m a m* edges [15], with the oxygen and nitrogen atoms arranged in accordance with theoretical predictions [16].

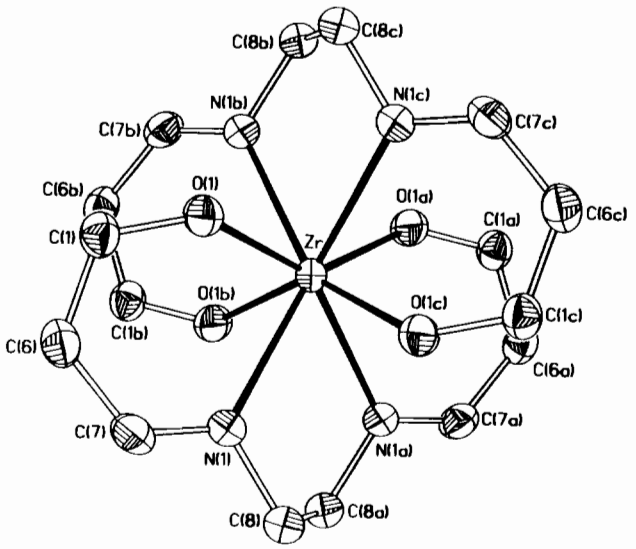

Fig. 1. ORTEP plot showing the Zr(*trans*-dsd)$_2$ atom numbering scheme and molecular structure, viewed along a direction which bisects the two perpendicular N,O,O,N planes.

*The angles between the normals to the triangular faces that are situated on each side of the four *b* edges [15] are the δ angles.

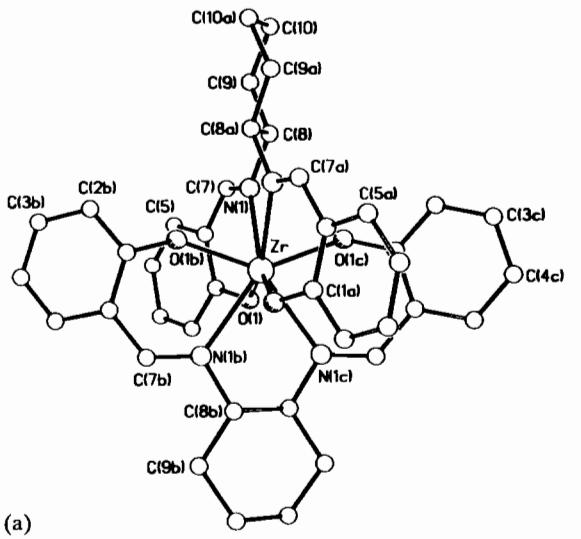

(a)

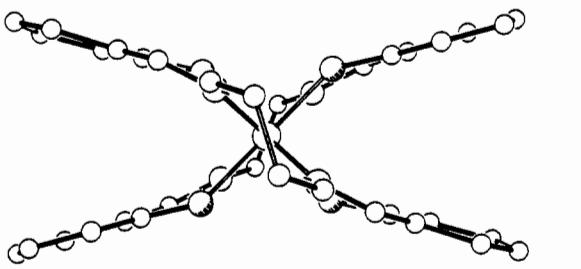

(b)

Fig. 2. (a) This orientation shows an approximately side-on view of one quadridentate ligand and a top view of the other ligand. (b) This view down one of the two fold axes, with cyclohexane rings omitted for clarity, shows the high point symmetry (D_2) of this molecule.

An additional noteworthy point is that the pseudo three fold rotation axes of the cyclohexane rings make an angle of 8.9° with the trapezoidal dihedral planes.

Bond length and angle values for Zr(*S,S-trans*-dsd)$_2$ benzene solvate are comparable to those of racemic Zr(*trans*-dsd)$_2$, but are less uniform. The space group of the former is only $P\bar{1}$ compared to *Fddd* for the latter. See also 'Supplementary material'.

Variable temperature ^{1}H NMR

Only the spectra of Zr(*cis*-dsd)$_2$ display significant temperature induced changes, so these spectra are included in Figs. 3 and 4. In contrast, only very subtle changes can be detected in the variable temperature ^{1}H NMR spectra for the other two complexes, and they can be described as follows: For Zr(dsp)$_2$, a second imine proton singlet, 0.03 ppm downfield and only *c.* 10% of the intensity of the other imine singlet, is apparent at 165.9 °C, but the signal broadens out and then reappears as two small singlets (8.54 and 8.46 ppm) by −37.4 °C. For Zr(*trans*-dsd)$_2$, the imine proton

TABLE 4. Selected bond distances (Å) for the coordination sphere of Zr(*trans*-dsd)$_2$[a]

Distances[b]			
Zr–O(1)	2.084(2)	C(6)–C(7)	1.451(3)
Zr–N(1)	2.423(2)	C(7)–N(1)	1.286(3)
O(1)–C(1)	1.315(3)	N(1)–C(8)	1.486(3)
C(1)–C(6)	1.421(3)	C(8)–C(8a)	1.542(5)
Angles[b]			
O(1)–Zr–O(1a)	139.7(1)[c]	N(1)–Zr–N(1a)[c]	70.3(1)
O(1)–Zr–O(1b)	97.9(1)	N(1)–Zr–N(1b)	130.2(1)
O(1)–Zr–O(1c)	95.7(1)	N(1)–Zr–N(1c)	133.8(1)
O(1)–Zr–N(1)	75.0(1)		
O(1)–Zr–N(1a)	145.2(1)	Zr–O(1)–C(1)	134.6(1)
O(1)–Zr–N(1b)	72.9(1)		
O(1)–Zr–N(1c)	74.4(1)	Zr–N(1)–C(7)	125.7(1)
		Zr–N(1)–C(8)	114.8(1)

[a]E.s.d.s are indicated in parentheses; atoms are labeled to agree with Fig. 1. [b]As required by symmetry, analogous bond lengths and angles elsewhere in the coordination sphere have exactly the same values (to within the e.s.d.s) as those reported in this Table. [c]Used to calculate $\theta_A = 35.2°$ (33.4°) and $\theta_B = 69.9°$ (73.0°) [15]. The values in parentheses are θ_A and θ_B values for Zr(dsp)$_2$ [11]. The hard sphere model predicts 36.9° and 69.5°, and the most favorable model predicts 35.2° and 73.5 °C, respectively [15].

TABLE 5. Dodecahedral edges in the Zr(*trans*-dsd)$_2$ coordination sphere

Edge[a]	Edge length (Å)	Edge[a]	Edge length (Å)
a Edges[b]			
N(1)–N(1a)	2.789	N(1b)–N(1c)	2.789
		mean	2.789
b Edges[b]			
O(1)–O(1b)	3.143	O(1a)–O(1c)	3.143
O(1b)–O(1a)	3.090	O(1c)–O(1)	3.090
		mean	3.117
g Edges[b]			
O(1)–N(1b)	2.690	O(1a)–N(1c)	2.690
O(1)–N(1)	2.757	O(1a)–N(1a)	2.757
O(1b)–N(1b)	2.757	O(1c)–N(1c)	2.757
O(1b)–N(1)	2.690	O(1c)–N(1a)	2.690
		mean	2.724
m Edges[b]			
O(1)–N(1c)	2.739	N(1a)–O(1b)	2.739
N(1)–O(1c)	2.739	N(1b)–O(1a)	2.739
		mean	2.739
Edge length ratios			
$b/a = 1.12$			
$b/m = 1.14$			
$b/g = 1.14$			

[a]Atoms are labeled as shown in Fig. 1. [b]Standard Hoard and Silverton symbolism [15].

is a singlet at 165.8 °C, which develops a downfield shoulder by 155.0 °C, and becomes a well resolved singlet at room temperature (0.02 ppm downfield from

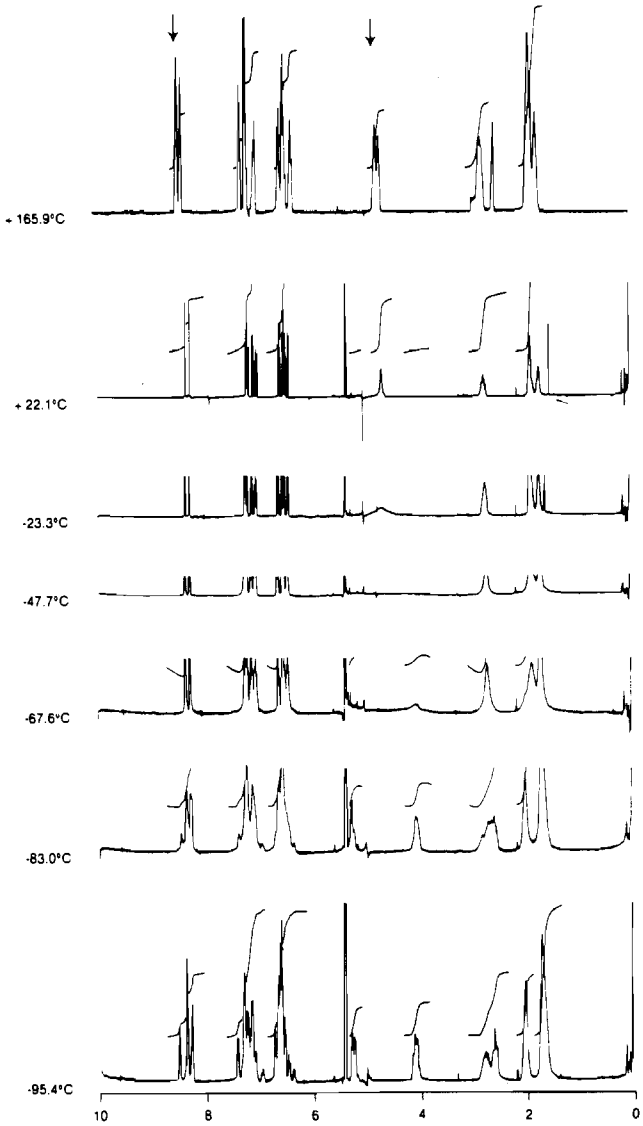

Fig. 3. The 400 MHz ^{1}H NMR spectra of Zr(*cis*-dsd)$_2$ in DMSO-d_6 (165.9 °C) and CD_2Cl_2 at various temperatures. Note in particular the changes in the 8.4 and 4.6 ppm regions.

the larger signal, and *c.* 30% of its intensity); other downfield 'shadows' of the larger signals appear concurrently, see Table 3. The 'shadows' become separated from the larger signals by *c.* 0.07 ppm by −93.6 °C.

Conformational analyses

The rate constants for the cyclohexane ring interconversion derived from the simulations are presented in Fig. 5. They were substituted into the Eyring equation

$$k = \frac{\kappa k_B T}{h} \exp((-\Delta^{\neq} + T\Delta^{\neq})/RT)$$

with the transmission coefficient, taken to be unity [17]. The best overall fit of $\ln(hk/k_BT)$ to T^{-1} gives $\Delta H^{\neq}$, $\Delta S^{\neq}$ and $\Delta G^{\neq}$ (298 K) equal to 27 ± 3 kJ mol^{-1}, -66 ± 13 J mol^{-1} K^{-1} and 46.5 ± 0.9 kJ mol^{-1}, re-

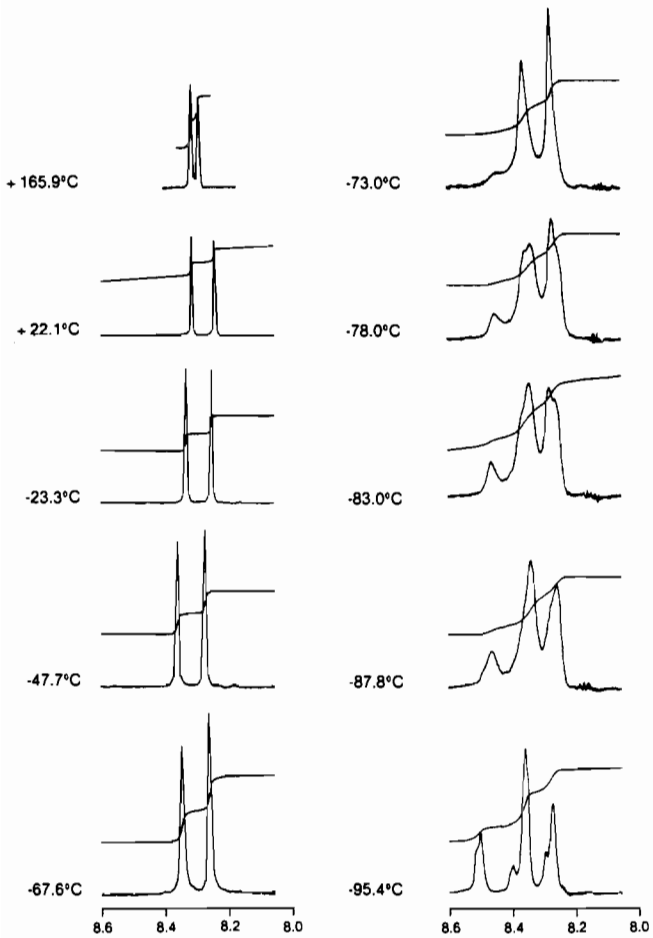

Fig. 4. The imine proton region, expanded, for the Zr(*cis*-dsd)$_2$ low temperature ramp; see Fig. 3. Note that the imine proton signal from one salicylidene arm broadens out before the other upon going to lower temperatures, and that apparently six imine signals (at least) result by −95.4 °C.

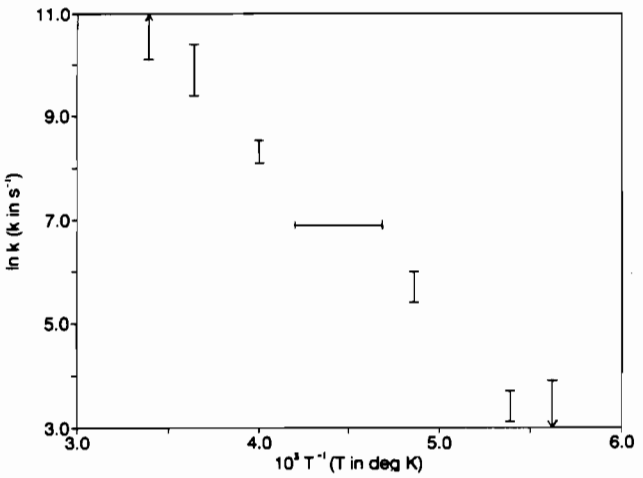

Fig. 5. Arrhenius plot for the cyclohexane ring interconversion of Zr(*cis*-dsd)$_2$. The rate constant at the coalescence temperature (1×10^3 s^{-1}) was calculated using the relation

$$k = \pi(\nu_A - \nu_x)/\sqrt{2}$$

where $(\nu_A - \nu_x)$ is the chemical shift difference in the absence of exchange and was also obtained from computer simulation. For fitting to the Eyring equation, the coalescence k was plotted as $\ln(kh/k_BT)$ vs. $1/T$ over the temperature range 213–238 K.

spectively. The most reliable value of $\Delta G^{\ddagger}$ is obtained at the coalescence temperature; $\Delta G^{\ddagger}$ (226 K) is 41.8 ± 0.1 kJ mol^{-1}. All uncertainty limits were obtained by drawing extreme lines through plots of the data.

Discussion

Synthesis and characterization

The reaction of Zr(O-n-Bu)$_4$·n-BuOH with a premade Schiff base (1:2), which is known to be a successful route to bis(quadridentate)zirconium(IV) complexes for Schiff bases made from 1,2-phenylenediamines [1a, 18], has now been extended to Schiff bases made from chiral (*R,R*- and *S,S*-) and meso (R,S-) cyclohexanediamines. All physical characterizations of these products, including elemental analysis, IR, UV–Vis, ^{1}H NMR, ^{13}C NMR, optical rotation, and the X-ray crystal structures of racemic Zr(*trans*-dsd)$_2$ and Zr(*S,S-trans*-dsd)$_2$, compare well with the H$_2$dsp/Zr(dsp)$_2$ system (both analyzed by X-ray crystallography [11, 19]) and are consistent with the proposed formulations for Zr(*cis*-dsd)$_2$, Zr(*R,R-trans*-dsd)$_2$ and Zr(*S,S-trans*-dsd)$_2$, *vide infra*.

Infrared

Upon coordination to zirconium, the IR spectra of the free ligands *cis*-H$_2$dsd and (±)*trans*-H$_2$dsd each undergo similar changes to that of H$_2$dsp [11], including a shift in the phenyl-to-oxygen vibrational frequency from *c.* 1280 to *c.* 1320 cm^{-1} and the loss of the broad O–H peak at 3400–3600 cm^{-1}. The imine bond vibrational frequency at *c.* 1630 cm^{-1} [20] characteristically undergoes little change as a result of this process [11].

UV–Vis

The free ligands display two broad bands in methylene chloride with wavelength maxima slightly shorter and molar absorptivities slightly smaller than H$_2$dsp (29 900 and 36 900 cm^{-1}, log ϵ values 4.28 and 4.37, respectively [11]). These bands are typically assigned to imine $\pi \rightleftharpoons \pi^*$ (lower energy) and aromatic $\pi \rightleftharpoons \pi^*$ (higher energy) transitions [10A]. Upon complexation to zirconium, the imine band goes to even lower energy and the aromatic band goes to even higher energy, and their molar absorptivities both increase slightly. Once again, the changes are similar to those seen for H$_2$dsp/Zr(dsp)$_2$

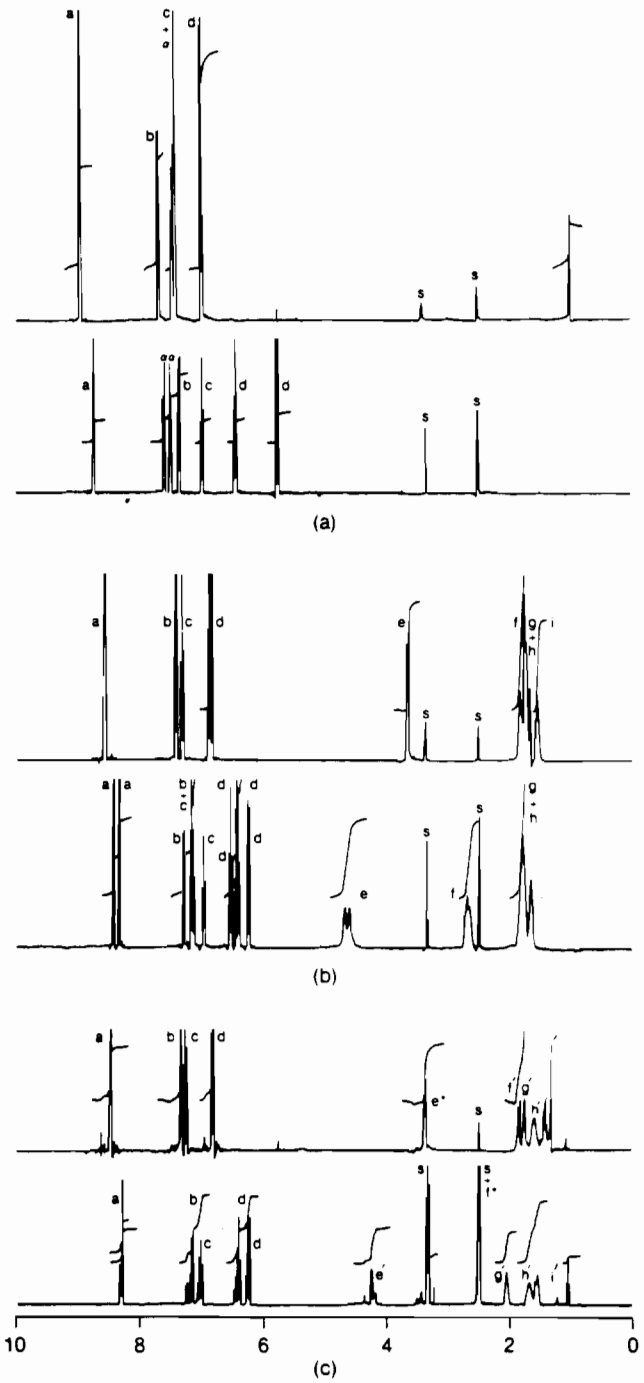

Fig. 6. Ambient temperature ^{1}H NMR spectra and assignments for: (a) top, H_2dsd; bottom, Zr(dsp)$_2$; (b) top, *cis*-H_2dsd; bottom, Zr(*cis*-dsd)$_2$; (c) top, *trans*-H_2dsd; bottom Zr(*trans*-dsd)$_2$. Assignments: a = imine proton, singlet; b–d = salicylidene ring protons that are *ortho* (doublet), *para* (triplet) and *meta* (triplet) to the oxygen donor atom, respectively; α = diamine ring protons, multiplet; e–h = cyclohexane ring axial and equatorial protons that are averaged by fast interconversion and are: on the carbon atoms alpha to the nitrogen donor atoms (e), two of the four protons on the beta carbon atoms (f), the other two protons on the beta carbon atoms and two protons of the gamma carbon atoms (g + h), and the other two protons on the gamma carbon atoms (i); e′–i′ = cyclohexane ring protons that are: on the carbon atoms alpha to the nitrogen donor atoms (e′), on the beta carbon atoms and equatorial (f′), on the gamma carbon atoms and equatorial (g′), on the beta carbon atoms and axial (h′), on the gamma carbon atoms and axial (i′); and s = solvent protons. The e* and f* signals can be observed at these chemical shifts in the $CDCl_3$ spectra of these compounds. The O–H regions for the free ligands at *c.* 13 ppm are not shown.

except that a third band (34 400 cm^{-1}) becomes apparent for the Zr(dsp)$_2$ complex [11]. Fortunately, this difference can be readily attributed to the diamine aromatic $\pi \rightleftharpoons \pi^*$ transition, which would be shifted differently than the salicylidene aromatic $\pi \rightleftharpoons \pi^*$ due to the different magnitude (compare Zr–N versus Zr–O bond distances, Table 4) and type [16] of interaction of the nitrogen versus oxygen donor atoms with the zirconium, and which would be absent from the cyclohexanediamine Schiff base complexes.

Ambient temperature ^{1}H NMR

Assignments for Zr(dsp)$_2$ [11], Zr(*cis*-dsd)$_2$, Zr(*trans*-dsd)$_2$ and their free ligands are given in Fig. 6, and in Figs. 1s and 2s (expanded aromatic regions and expanded cyclohexane regions, respectively), see 'Supplementary material'. Due to the complete resolution of the aromatic proton signals for each complex, these assignments could definitively be made based on chemical shifts, peak integration and multiplicities. Unfortunately, the cyclohexane proton signals of Zr(*cis*-dsd)$_2$ and Zr(*trans*-dsd)$_2$ are not as readily assignable due to the different conformational behavior of their aliphatic rings, and therefore will be discussed later.

The changes that take place in the ^{1}H NMR spectra when the H_2dsd free ligands become coordinated are comparable to those of H_2dsp in that the phenoxy proton signal vanishes, the imine proton signal is shifted upfield *c.* 0.15 ppm, and the salicylidene aromatic proton signals are all shifted upfield to varying extents with the *meta* {adjacent to the imine bond} proton doublet being shifted the most. Another obvious trend upon coordination is that the cyclohexanediamine ring protons all move downfield to varying extents, as do the aromatic diamine protons of Zr(dsp)$_2$. These observations can be explained as follows: As the zirconium(IV) ion replaces the phenoxy protons of each ligand, its predominant effects are (i) σ-inductive electron withdrawal from the nitrogen donor atoms, causing deshielding of the diamine ring protons, and (ii) π-electron withdrawal from the salicylidene system, resulting in a diminished ring current, less deshielding, and an upfield shift even for the imine proton. This explanation is consistent with theory, which predicts that the B sites of a dodecahedron (occupied by the oxygen atoms) should prefer the better π-donors and the A sites (occupied

by the imine nitrogen atoms) should prefer the better π-acceptors for a d^0 ion [16].

Some points of interest about the individual spectra are included with 'Supplementary material'.

$^{13}C\{^1H\}$ NMR

Signal assignments for all ligands and complexes are also definitive. For H_2dsp and Zr(dsp)$_2$ there are 10 signals, one for each carbon, all reasonably attributed to aromatic and imine carbons. The farthest downfield signal is assigned to the two salicylidene carbons having the oxygen substituents, followed by a signal due to the imine carbons which are bonded to the less electronegative nitrogens (see Table 3). The three signals attributed to the aromatic diamine carbons (α, β, and γ to the nitrogen atoms) were identified by their absence from the dsd(2−) spectra, and are found at 146(142), 127(127) and 120(119) ppm, respectively, for the complex, with H_2dsp values in parentheses. The remaining signals at 134(133), 133(132), 122(119.7), 119(119.2), 116(117) ppm are assigned to the salicylidene carbons *ortho* (2), *para* (1) and *meta* (2) to the oxygen.

Assignments for the salicylidene carbons of the dsd(2−) ligands and complexes follow this same pattern. As for the diamine moiety, the cyclohexane carbons are of three general types (α, β, γ) and are typically assigned according to their proximity to the nitrogens [2e–g, 7a, c, 22b, 21].

The changes in the $^{13}C\{^1H\}$ NMR that take place upon coordination of the free ligands to zirconium(IV) are not very dramatic and few general trends are seen. The salicylidene carbons *para* to the oxygen substituents move downfield *c.* 3–4 ppm in all three cases, which is consistent with the π-electron-withdrawing nature of the dodecahedral B sites for a d^0 ion [16]. Also, the β-carbons of the cyclohexane rings move upfield in both of these cases (2.1 and 2.6 ppm). The primary reason for this scarcity of trends upon coordination is that rapid cyclohexane ring inversion is likely for both free ligands and Zr(*cis*-dsd)$_2$ (next section) producing averaged signals, but that averaged signals are not likely for the 'locked' Zr(*trans*-dsd)$_2$.

One other point of interest regarding the $^{13}C\{^1H\}$ NMR spectra of these complexes is that most of the carbon signals for Zr(*trans*-dsd)$_2$ also exist as pairs, as for Zr(*cis*-dsd)$_2$, but with a separation between the signals of each pair of only *c.* 0.1 ppm. Since the signal from the imine carbons is *not* one of the split signals, an alternative to the 'different salicylidene moiety' explanation is required. The *trans* complex was originally made from non-optically resolved cyclohexanediamine, which means that both *R,R-trans*-H_2dsd and *S,S-trans*-H_2dsd were present at the time of complexation, and that *R,R-R,R, S,S-S,S* and *R,R-S,S* ligand combinations were possible for Zr(*trans*-dsd)$_2$. In order to determine if these isomers are responsible for the pairs of signals observed, the optically resolved complexes were prepared from the optically pure diamines, and their spectra were obtained both separately and together, in $CDCl_3$ solution. No separated signals were observed for any of the latter three spectra, conclusively indicating that the Zr(*R,R-trans*-dsd)(*S,S-trans*-dsd) complex was the source of the signals finely separated from those of the enantiomers Zr(*R,R-trans*-dsd)$_2$ and Zr(*S,S-trans*-dsd)$_2$. Different orientations of chiral ligands have already been shown to cause small ^{13}C NMR signal separations in other systems [2d, f].

Optical rotation

Characterization of *R,R-trans*-H_2dsd and *S,S-trans*-H_2dsd (as oils) and their complexes by optical rotation indicated that the diamine's direction of rotation of the plane polarized light was retained upon formation of the Schiff base, as previously observed [10c], and was changed upon formation of the zirconium complexes, as observed for other complexes [2a, 3c, 10a, 22].

Thermogravimetric analysis

The higher thermal stability of the racemic Zr(*trans*-dsd)$_2$ complex versus the Zr(*cis*-dsd)$_2$ complex (see Table 3), can also be understood in light of the X-ray crystal structure results. The highly symmetrical packing arrangement of the former is likely to produce a higher lattice energy than the latter, which in turn would account for the greatly reduced solubility observed for the former in methylene chloride, chloroform and dimethyl sulfoxide. The literature also indicates that *trans*-DACH complexes are generally more stable than *cis*-DACH complexes [23] and that *cis*-DACH complexes may be more strained [7a]. The thermal stabilities of both zirconium complexes are only modestly less than those for Zr(dsp)$_2$ whose onset of weight loss is 380 °C in N_2(g) and 405 °C in air (see Table 3).

X-ray crystal structure

Crystals suitable for single crystal X-ray diffraction analysis were readily obtained from cold methylene chloride solution for Zr(*S,S-trans*-dsd)$_2$ and from benzene–pet. ether (B) for Zr(*trans*-dsd)$_2$, but were not obtained for Zr(*cis*-dsd)$_2$. Suitable single crystals have been obtained for other complexes containing *cis*-dsd(2−) [24] and *cis*-DACH [2h, 25], however, so efforts to grow crystals of Zr(*cis*-dsd)$_2$ are continuing.

The Zr–O and Zr–N bond lengths obtained from these structure determinations are comparable to those in analogous bis(quadridentate)zirconium complexes derived from aromatic diamines [1a, 11], which means

that the hybridization of the diamine α-carbons (sp^2 for dsp versus sp^3 for dsd) apparently has either very little or no effect on the Zr–N bonds. Their uniformity, however, in the racemic Zr(*trans*-dsd)$_2$ is unprecedented for this type of complex as is the molecular point symmetry, D_2 [1a, 11]*.

The three parameters that traditionally determine the dodecahedral shape, θ_A, θ_B and Zr–N(av.)/Zr–O(av.) [15], have values of 35.2°, 69.9° and 1.16 for the racemic Zr(*trans*-dsd)$_2$ structure, respectively. These numbers are interesting in that, while the bond length ratio is comparable to those for previous structures [1a, 11], the angles more closely resemble the hard sphere model [15] and most favorable model [15] than those for the previous structures (see Table 4). Another distinctive aspect for the molecular shape of this complex is that the dodecahedral *m* edges are virtually equal in length to the *g* edges, and very close to the *a* edge length as well, which likewise is consistent with the hard sphere model [15].

Structural aspects concerning the ligands include: (i) the larger distortions from planarity for the donor atoms of each ligand, by a factor of 2 to 3 as compared to Zr(dsp)$_2$ [11], (ii) the longer (by 0.11 Å) dodecahedral *a* edges versus Zr(dsp)$_2$ [11], due to the non-aromatic diamine ring moiety (sp^3–sp^3 overlap), (iii) the perpendicular orientation of the donor atom planes for each ligand, as for Zr(dsp)$_2$, (iv) the highly localized imine double bond [3f, 11, 24], and (v) the fact that the largest torsional angles arise from rotation about the diamine ring-to-nitrogen bond, as was the case in previous single crystal structures [1a, 11].

Variable temperature NMR

The ^{1}H NMR spectra of Zr(*cis*-dsd)$_2$, Zr(*trans*-dsd)$_2$ and Zr(dsp)$_2$ were obtained at various temperatures between 165.9 and 19.9 °C in DMSO-d_6 and at various temperatures between 22.1 and −95.4 °C in CD_2Cl_2 in order to identify which signals represent averaged proton environments and to deduce which rapid molecular motions are responsible. The only general observation that applies to the spectra of each complex upon going from high to low temperatures is that the smaller coupling details become obscured, presumably because of increasing viscosity of the solvent. There was no positive evidence for rapid ligand exchange at high temperatures for any of the complexes [26], unlike complexes reported previously [8c, 9]. However, there were no peaks assignable to ^3J(Zr–H) or ^4J(Zr–H) for ^{91}Zr (I=5/2, 11.23% abundant) in any of the spectra.

Zr(cis-dsd)$_2$–cyclohexane ring

The broadening of the methine proton signals (4.6 ppm, 22.1 to −47.7 °C) and reappearance of two signals approximately equidistant from the high temperature signal (5.2 and 4.1 ppm, −67.6 to −95.4 °C; see Fig. 3) firmly establishes that the cyclohexane ring of Zr(*cis*-dsd)$_2$ undergoes rapid interconversion with $\lambda \rightleftharpoons \delta$ interconversion of the five-membered ring on the NMR time scale at or above ambient temperature [2b, 7]**, and that the averaged axial and equatorial methine signals are able to be resolved at low temperature. The upfield methine signal (4.1 ppm) can confidently be assigned to the axial methine proton on the basis of its similar chemical shift to that of the methine proton signal of Zr(*trans*-dsd)$_2$, 4.2 ppm (see Table 3). The latter signal shows no analogous changes over the entire temperature range studied, which is consistent with a conformationally locked [2b, 3d, 4a, 10] complex where the donor atoms occupy the equatorial positions and methine protons, therefore, occupy the *axial* positions.

The different shapes of the resolved methine signals are attributed to the different coupling experienced by the slowly exchanging axial proton ($^3J_{ax-eq}$ from the other methine proton, $^3J_{ax-ax}$ and $^3J_{ax-eq}$ from the β-carbon protons) versus the equatorial proton ($^3J_{eq-ax}$ from the other methine proton, $^3J_{eq-ax}$ and $^3J_{eq-eq}$ from the β-carbon protons). Thus these shapes also corroborate the above assignments because $^3J_{ax-ax}$ is typically larger than $^3J_{eq-ax}$ or $^3J_{eq-eq}$ (for $^3J_{ax-ax}$, $^3J_{ax-eq}$ and $^3J_{eq-eq}$, the ranges are 8–10, 2–3 and 2–3 Hz, respectively [27]), and the upfield signal is the broader one. This assignment also is in agreement with previous assignments in which the equatorial proton is considered to be downfield from the axial [27a, 28].

However, the actual splittings of the peaks in each of the resolved methine signals, *c.* 20 Hz peak to peak distance, are somewhat larger than those usually attributed to coupling alone [27a]†. It is likely that the different salicylidene moieties, which make the α-carbons different in the ^{13}C NMR (see Table 3) even when averaged at ambient temperature, are contributing to this splitting. This effect could also account for the large methine peak splitting observed in DMSO-d_6 at high temperature, *c.* 25 Hz, where the vicinal coupling constants should be time averaged to $0.5[(^3J_{ax-ax}+4(^3J_{ax-eq})+{}^3J_{eq-eq})]$. This value is only 13 Hz for 'salicylidene-less' *cis*-DACH coordinated to Pt^{2+} [2c]. (This expression will be smaller by $2(^3J_{ax-eq})$ when the methine signals are equated by rapid motion.)

*Likewise, the δ angles [14] are all uniform (22.70) and comparable in size to the other complexes [1a, 11]. The Zr–N–C(imine) and Zr–N–C(ring) bond angles are also uniform and comparable [1a, 11].

**Solvent also appears to play a role in the averaging process, since the methine region of the ambient temperature DMSO-d_6 spectrum displays sharp signals, resembling the high temperature averaged signals, in contrast to the ambient temperature CD_2Cl_2 which shows more broadening.

†$^3J_{ax-ax}$=11 Hz for [Fe(CN)4*R*,*R*-*trans*-DACH] [27a].

In addition to resolving the methine protons, the low temperature ^{1}H NMR spectra of Zr(*cis*-dsd)$_2$ also resolve the axial and equatorial protons of the β- and γ-carbons. Assignment of these low temperature signals was possible by using models and the equatorial-downfield-from-axial principle, and these assignments in turn were used to substantiate the assignments of the averaged signals in the high temperature spectra (see Fig. 6).

The thermodynamic values obtained for the cyclohexane ring interconversion of Zr(*cis*-dsd)$_2$ invite comparisons to those of cyclohexane ($\Delta G^{\ddagger} = 42.1$ kJ mol^{-1} at 298 K, $\Delta H^{\ddagger} = 44.8 \pm 0.2$ kJ mol^{-1}, $\Delta S^{\ddagger} = 9.2 \pm 0.8$ J mol^{-1} K^{-1}) [5b] and Fe(CN)$_4$(*cis*-DACH) ($\Delta G^{\ddagger} = 45.0$ kJ mol^{-1} at 298 K, $\Delta H^{\ddagger} = 42.7 \pm 2.0$ kJ mol^{-1}, $\Delta S^{\ddagger} = -7.7 \pm 8.4$ J mol^{-1} K^{-1}) [7b].

Given the large differences in these three compounds, it is remarkable that their $\Delta G^{\ddagger}$ values are so close, indicating that the probability of an interconversion is almost the same in each compound, and that the rate constants describing the motion, spanning approximately three orders of magnitude over a 120 °C temperature range for Zr(*cis*-dsd)$_2$, are also comparable. The observation that different metal ions have little impact on $\Delta G^{\ddagger}$ for complexes with the same diamine ligands, due to offsetting effects, has already been made [7b, 29].

In comparing the $\Delta H^{\ddagger}$ of the iron complex to the much lower $\Delta H^{\ddagger}$ of the zirconium complex, a factor to consider is the strain caused in the five-membered rings as a function of the metal–nitrogen bond length. To evaluate this ring strain, Hawkins *et al.* proposed that (i) the five-membered chelate ring can be considered to be the sum of an N–M–N fragment and an N–C–C–N fragment [29], and (ii) since an undistorted envelope conformation requires an N–N distance of 252 pm for the N–C–C–N fragment [29], the extent to which the N–N distance of the N–M–N fragment differs from this value will determine the ring strain. In the octahedral iron complex, the Fe–N distance can be minimally estimated to be 194 pm [10d, 27, 30]* giving minimum N–N distance of 274 pm. In the eight-coordinate zirconium complex, the Zr–N bond length is 242 pm and the N–Zr–N angle is 70.3° (see Table 4) giving an N–N distance of 279 pm. Thus, there is a comparable mismatch between the two fragments in the zirconium complex and in the iron complex, which should lead to comparable ring strain. However, the nitrogens in the zirconium *cis*-dsd complex are sp^2 hybridized (120° preferred bond angles), while those in the iron DACH complex are sp^3 hybridized (109° preferred bond angles). Thus we hypothesize that the N–C–C–N of the *cis*-dsd ligand will accommodate oversized N–M–N fragments with less strain than the N–C–C–N of *cis*-DACH. Although this effect is in the right direction, it is probably of insufficient magnitude to explain the large difference in $\Delta H^{\ddagger}$ between the two compounds [29].

Although large positive or negative values of $\Delta S^{\ddagger}$ (those outside the range of ± 42 J mol^{-1} K^{-1}) are considered unlikely for conformational processes in rings [5b], it is possible to rationalize a large negative value in a complex by considering the relative masses of the interconverting rings and the substituents enjoined by the motion. In cyclohexane, ring interconversion requires no translational motion. In the iron complex, the interconversion of the six-membered ring requires offsetting through-space motions of both the ring and the Fe(CN)$_4$ component. In the zirconium complex, however, the zirconium center and one of its quadridentate ligands is so much heavier than the interconverting ring on the other ligand that the center remains approximately at rest, and causes the six-membered ring to make large excursions through space in order to interconvert. If the transition state is very well defined compared to the ground state, then $S^{\ddagger} \ll S_{eq}$, and $\Delta S^{\ddagger} = S^{\ddagger} - S_{eq}$ is large and negative (where S_{eq} is the entropy of the ground state). In addition, the salicylidene moieties attached to the five-membered chelate rings of Zr(*cis*-dsd)$_2$ are also likely to exert an influence on the ring interconversion, as mentioned for $\Delta H^{\ddagger}$. Therefore it is not unreasonable that the $\Delta S^{\ddagger}$ for this compound differs significantly from those for the other two compounds.

Zr(cis-dsd)$_2$–imine region

Upon reaching temperatures of -73.0 °C to -95.4 °C, the imine region of the Zr(*cis*-dsd)$_2$ complex does show additional splitting (Fig. 4), indicating that *each* of the two ambient temperature imine signals is actually an averaged signal due to rapid motion on the NMR time scale. Some of the general factors that can contribute to the inequivalence of these structurally similar salicylidene moieties include ring strain, steric effects and preferred donor atom sites. Two specific factors that may also contribute to the appearance of the six (or more) imine signals at low temperature are: (i) that the donor atoms of the *cis*-dsd(2−) ligand are capable of non-planarity [24], and (ii) that the chelate 'bite' sizes in Zr(*cis*-dsd)$_2$ should be comparable to Zr(*trans*-dsd)$_2$, and, therefore, comparable to the hard sphere model [15] where dodecahedral edge $m = a = g < b$ (see Table 5).

Considering all of the above factors, the theoretical preference of eight-coordinated d^0 ions with different donor atoms for the dodecahedron [16], and the X-ray crystal structure results for other bis(quadridentate

*If significantly different, the Fe(II)–N bond distance would be greater than the Co(III)–N bond distance, and the N–N distance would be even larger.

Schiff base)zirconium(IV) complexes [1a, 11], the presence of different isomers which arise from different salicylidene conformations or ligand wrapping (geometric isomerism) is possible. If the chelate bites are restricted to the *m*, *a* and/or *g* edges, and if the dsd(2−) ligands are not permitted to be very far from planarity, then the two most probable geometric isomers are an *m,a,m–m,a,m* isomer of D_{2d} donor atom symmetry and an *m,g,g–g,g,m* isomer of C_2 donor atom symmetry (which has an enantiomer). In the former isomer the donor atoms of each ligand are coplanar. However, since the cyclohexane ring is interconverting slowly on the NMR time scale at −95.4 °C, the salicylidene moieties bonded to axial nitrogen atoms versus equatorial nitrogen atoms are likely to be distinguishable, and two imine signals should be produced. In the latter isomer the two salicylidene moieties of each ligand span different dodecahedral edges and are therefore symmetry inequivalent. Again, the salicylidene moieties bonded to axial versus equatorial nitrogen atoms should be distinguishable at −95.4 °C, so four signals should result from this isomer (e.g. axial-*m* edge, equatorial-*m* edge, axial-*g* edge and equatorial-*g* edge). Thus, a total of six signals would be expected, which is equal to the number observed. Furthermore, two averaged salicylidene sets of signals would be expected from the rapid interconversion on the NMR time scale of the *m,a,m–m,a,m* and *m,g,g–g,g,m* isomers, one salicylidene intermediate between *m* and *m* edges and the other between *m* and *g* edges, which is consistent with observations at temperatures of −67.6 °C and above.

However, if the two postulated geometric isomers are the only ones present at −95.4 °C, (i) their relative amounts should reflect their relative stabilities and (ii) three *pairs* of imine signals should be evident, with both pairs from the C_2 isomer having the same integration. It is the latter criterion that does not appear to be met, as follows. The four smaller low temperature imine peaks would have to arise from the *m,g,g–g,g,m* isomer which would be present in lesser amount (two pairs of equal integration), and the two larger peaks would have to arise from the *m,a,m–m,a,m* isomer present in greater amount. These two larger peaks, however, make unconvincing partners due to their respective integrations.

Considerable support for an alternative comes from a preliminary 2-D NMR experiment (proton versus proton) which indicates that there is interaction between the imine protons and the cyclohexane ring protons whose chemical shifts are at 1.8–1.5 ppm. Thus, any geometrical isomer having different salicylidene moieties (such as the *m,g,g–g,g,m* isomer) would give two averaged imine signals at high temperature and a variety of imine signals at low temperature, depending on the preferred positions of the cyclohexane rings; i.e. conformational isomers for the Zr(*R,S-cis*-dsd)$_2$, Zr(*R,S-cis*-dsd)(*S,R-cis*-dsd) and Zr(*S,R-cis*-dsd)$_2$ may not produce the same imine signals at low temperature in this scenario (see 'Supplementary material'). Additional alternatives involving other geometric and/or polytopal isomers are also feasible.

Also note that, as the temperature is lowered, the downfield imine peak broadens before the other. If the downfield imine peak is resolved into peaks separated by a smaller chemical shift, this would indicate that the salicylidene environments change at different rates.

Zr(trans-dsd)$_2$

The ^{1}H NMR signals of Zr(*trans*-dsd)$_2$ at 165.8 °C, which are consistent with the presence of only one type of salicylidene moiety and one type of cylohexane ring, must be motionally averaged as well because small signals from a second type of salicylidene moiety become increasingly resolved at lower and lower temperatures. These resolved signals are not likely to be caused by a cyclohexane ring interconversion becoming slow on the NMR time scale because there is no broadening of the methine proton signal and no subsequent resolution into axial and equatorial signals. This observation is consistent with the notion that coordinated *trans-*

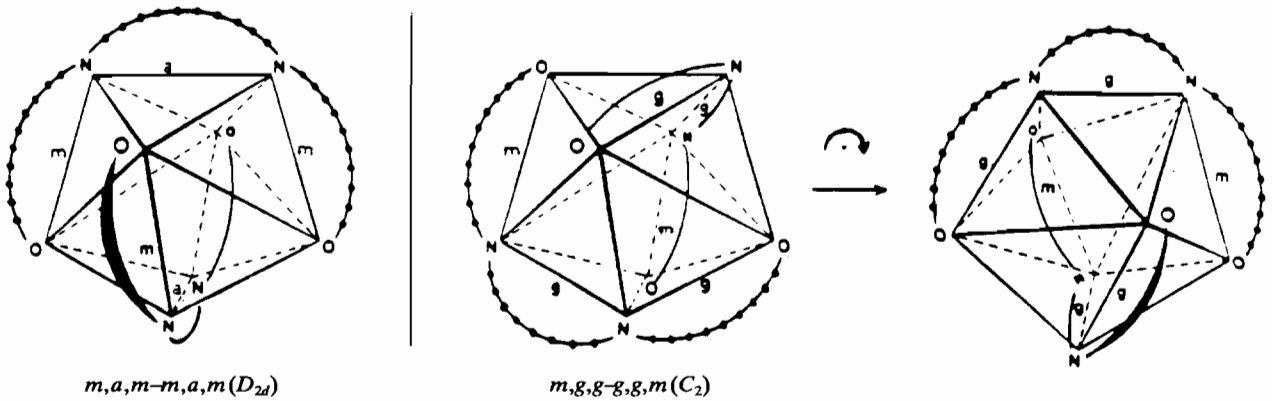

m,a,m–m,a,m (D_{2d}) *m,g,g–g,g,m* (C_2)

cyclohexanediamines are conformationally locked [2b, 3d, 4a, 10]. Therefore, since the donor atoms of *trans*-dsd(2−) can also be non-planar [3a–e, 4c], chelate ring strain, steric effects and preferred donor atom sites are once again likely to stabilize a second salicylidene orientation. A small amount of either a conformational isomer, a symmetrical geometric isomer or a symmetrical polytopol isomer could give rise to the additional set of salicylidene NMR signals.

Zr(dsp)$_2$

The presence of a small imine peak which is *more* clearly separated from the predominant imine peak in the 165.9 °C ^{1}H NMR spectrum, than in lower temperature spectra, and which is resolved into two signals by −37.4 °C, indicates that a small amount of a second species is present. Despite the capability of dsp(2−) to also assume non-planar donor atom arrangements*, this species is not likely to be a geometrical, conformational, or polytopol isomer of the predominant species since no averaging with the predominant NMR signals is observed. Since long term heating of Zr(dsp)$_2$ samples in NMR tubes do show significant change [32], the second species could be a solvolysis product formed during the temperature equilibration period. The DMSO solution stability of bis(quadridentate)-zirconium(IV) complexes is currently receiving further study.

Conclusions

Insights into the molecular motion of the title complexes include the following.

(1) The presence of two imine proton signals in the ambient temperature ^{1}H NMR of Zr(*cis*-dsd)$_2$ is not due to slow cyclohexane ring interconversion, although this reason was invoked previously to explain similar observations for other quadridentate Schiff base complexes of *cis*-DACH [8a]. Instead, interconversion of geometric, conformational and perhaps polytopal isomers produce different averaged chemical environments for the two salicylidene moieties of each ligand.

(2) Upon going to lower temperature, the interconversion of the cyclohexane rings in Zr(*cis*-dsd)$_2$ becomes slow on the NMR time scale, as evidenced by the resolution of the ambient temperature methine proton signal into axial (upfield) and equatorial (downfield) signals. The slowing of the cyclohexane ring interconversion, along with the slowing of the isomer interconversions, are responsible for the resolution of the two averaged imine signals into six signals upon reaching −95.4 °C.

(3) Since the averaged downfield imine signal of Zr(*cis*-dsd)$_2$ broadens at higher temperature than the upfield signal and yet is resolved into signals having an apparently smaller chemical shift separation, a measure of independence must exist for the molecular motions involving the two salicylidene moieties of each ligand. Thus, some independence of the salicylidene motions from the cyclohexane ring interconversion must exist as well.

(4) The similarity of $\Delta G^{\ddagger}$ for this complex to those for compounds such as cyclohexane [5b] and Fe(CN)$_4$(*cis*-DACH) [7b] is probably coincidental, since their $\Delta H^{\ddagger}$ and $\Delta S^{\ddagger}$ values do not agree. Some disagreement is expected due to the presence of the salicylidene substituents and several other factors.

(5) Upon going to lower temperatures, slowing isomer interconversion begins to play a role in the ^{1}H NMR of Zr(*trans*-dsd)$_2$ as well. However, the failure of its methine signal to become resolved into two signals suggests that the cyclohexane ring is indeed locked into a single conformation.

(6) Since Zr(dsp)$_2$ lacks cyclohexane rings and fails to give any additional salicylidene proton signals to −95.0 °C, information regarding its molecular motion was not obtained. Either the molecular motion remains fast on the NMR time scale, or isomers having different salicylidene chemical environments do not exist.

Supplementary material

Tables Is: crystal data for Zr(*trans*-dsd)$_2$, 2 pages; IIs: deviations in Å from least squares mean trapezoidal planes for the Zr(*trans*-dsd)$_2$ coordination sphere, 1 page; IIIs: torsional angles in coordinated *trans*-dsd(2−) ligands, 1 page; IVs: bond lengths for Zr(*trans*-dsd)$_2$, 1 page; Vs: bond angles for Zr(*trans*-dsd)$_2$, 1 page; VIs: anisotropic thermal parameters for Zr(*trans*-dsd)$_2$, 1 page; VIIs: hydrogen atom coordinates for Zr(*trans*-dsd)$_2$, 1 page; VIIIs: structure factors for Zr(*trans*-dsd)$_2$, 11 pages. IXs: all X-ray crystallographic data for Zr(*S,S-trans*-dsd$_2$, 26 pages. Figures 1s: ^{1}H NMR expanded aromatic region for all ligands and complexes, 5 pages; 2s: ^{1}H NMR expanded cyclohexane region for dsd(2−) ligands and complexes, 1 page; 3s: 2-D NMR (proton versus proton) for Zr(*cis*-dsd)$_2$, and some feasible low temperature isomers, 2 pages; 4s: ^{13}C NMR spectra for all ligands and complexes, including Zr(*R,R-trans*-dsd)$_2$ and Zr(*S,S-trans*-dsd)$_2$, 9 pages; 5s: thermograms for Zr(*cis*-dsd)$_2$ and Zr(*trans*-dsd)$_2$ under dinitrogen

*The dsp(2−) ligand can also assume a *β-cis* arrangement in octahedral complexes [31].

and under air, 4 pages, are available from the general correspondence author on request.

Acknowledgements

The authors are indebted to a number of organizations and programs for financial support. These include a RIT Dean's Summer Research Fellowship (M.L.I.), two RIT Graduate Student Scholarships (B.P.C.), the award by St. John Fisher College of a Sabbatical Leave (L.J.S.), and the RIT College of Science for funding the variable temperature NMR experimentation. We would also like to recognize Aidan Harrison and David Fuller of the Cornell University NMR Laboratory for expert technical assistance, Microlytics for some of the elemental analyses, and Fisons Corporation for additional instrumental analyses. And finally, we would like to thank Bristol-Myers for testing the antitumor activity of the new complexes (the tests were negative).

References

1 (a) M. L. Illingsworth and A. L. Rheingold, *Inorg. Chem., 26* (1987) 4312; (b) R. D. Archer and B. Wang, *Inorg. Chem., 29* (1990) 39.

2 (a) N. Farrell, D. M. Kiley, W. Schmidt and M. P. Hacker, *Inorg. Chem., 29* (1990) 397; (b) M. Gulloti, G. Pacchioni, A. Pasini and R. Ugo, *Inorg. Chem., 21* (1982) 2006; (c) K. Inagaki, H. Nakahara, M. Alink and Y. Kidani, *Inorg. Chem., 29* (1990) 4496; (d) T. K. Miyamoto, K. Okude, K. Maeda, H. Ichida, Y. Sasaki and T. Tashiro, *Bull. Chem. Soc. Jpn., 62* (1989) 3239; (e) P. Bitha, G. O. Morton, T. S. Dunne, E. F. Delos Santos, Y. Lin, S. R. Boone, R. C. Haltiwanger and C. G. Pierpont, *Inorg. Chem., 29* (1990) 645; (f) J. D. Hoeschele, N. Farrell, W. R. Turner and C. D. Rithner, *Inorg. Chem., 27* (1988) 4106; (g) M. Noji, K. Okamoto and Y. Kidani, *J. Med. Chem., 24* (1981) 508; (h) L. S. Hollis, A. R. Amundsen and E. W. Stern, *J. Am. Chem. Soc., 107* (1985) 274; (i) J. D. Page, I. Husain, A. Sancar and S. G. Chaney, *Biochemistry, 29* (1990) 1016; K. J. Miller, S. L. McCarthy and M. Krauss, *J. Med. Chem., 33* (1990) 1043; T. K. Miyamoto, K. Okude, K. Maeda, H. Ichida, Y. Sasaki and T. Tashiro, *Chem. Lett.*, (1989) 1377.

3 (a) Y. Fujii, K. Matsutani and K. Kikuchi, *J. Chem. Soc., Chem. Commun.*, (1985) 415; (b) Y. Fujii, K. Kikuchi, K. Matsutani, K. Ota, M. Adachi, M. Syoji, I. Haneishi and Y. Kuwana, *Chem. Lett.*, (1984) 1487; (c) K. Fujii, M. Matsufuru, A. Saito and S. Tsuchiya, *Bull. Chem. Soc. Jpn., 54* (1981) 2029; (d) Y. Fujii, M. Sano and Y. Nakano, *Bull. Chem. Soc. Jpn. 50* (1977) 2609; (e) K. Fujii and M. Sano, *Chem. Lett.*, (1976) 745; (f) M. A. Cox, T. J. Goodwin, P. Jones, P. A. Williams, F. S. Stevens and R. S. Vagg, *Inorg. Chim. Acta, 127* (1987) 49.

4 (a) M. Saburi and Y. Sadao, *Bull. Chem. Soc. Jpn., 47* (1974) 1184; (b) J. F. Resch and J. Meinwald, *J. Tetrahedron Lett., 22* (1981) 3159; (c) K. Fujii, Y. Yoshikawa, M. Syoji and H. Shinohara, *Bull. Chem. Soc. Jpn., 63* (1990) 138; (d) T. Mizuta, K. Toshitani, K. Miyoshi and H. Yoneda, *Inorg. Chem., 29* (1990) 3020; S. C. Benson, P. Cai, M. Colon, M. A. Haiza, M. Tokles and J. K. Snyder, *J. Org. Chem., 53* (1988) 5335.

5 (a) K. Tatsumi, I. Matsubara, Y. Inoue, A. Nakamura, R. E. Cramer, G. J. Tagoshi, J. A. Golen and J. W. Gilje, *Inorg. Chem., 29* (1990) 4928; (b) L. M. Jackman and F. A. Cotton (eds.), *Dynamic Nuclear Magnetic Resonance Spectroscopy*, Academic Press, New York, 1975; (c) C. J. Hawkins and J. A. Palmer, *Coord. Chem. Rev., 44* (1982) 1.

6 R. C. Fay and J. K. Howie, *J. Am. Chem. Soc., 99* (1977) 8110.

7 (a) T. Lind and H. Toftlund, *Acta Chem. Scand., Ser. A, 36* (1982) 489; (b) Y. Kuroda, N. Tanaka, M. Goto and T. Sakai, *Inorg. Chem., 28* (1989) 997; (c) *Inorg. Chem., 28* (1989) 2163.

8 (a) G. C. van Stein, G. van Koten, K. Vrieze, C. Brevard and A. L. Spek, *J. Am. Chem. Soc., 106* (1984) 4486; (b) G. C. van Stein, G. van Koten, K. Vrieze, A. L. Spek, E. A. Klop and C. Brevard, *Inorg. Chem., 24* (1985) 1367; (c) G. C. van Stein, G. van Koten, K. Vrieze and C. Brevard, *Inorg. Chem., 23* (1984) 4269.

9 Y. Ba, R. Song and Z. Qui, *Magn. Reson. Chem., 27* (1989) 916.

10 (a) A. Pasini, M. Gulloti and R. Ugo, *J. Chem. Soc., Dalton Trans.*, (1977) 346; (b) E. Cesarotti, M. Gulloti, A. Pasini and R. Ugo, *J. Chem. Soc., Dalton Trans.*, (1977) 757; (c) H. Aoi, M. Ishimori, S. Yoshikawa and T. Tsuruta, *J. Organomet. Chem., 85* (1975) 241; (d) M. Takata, K. Kashiwabara, H. Ito, T. Ito and J. Fujita, *Bull. Chem. Soc. Jpn., 58* (1985) 2247; (e) E. Cesarotti, A. Pasini and R. Ugo, *J. Chem. Soc., Dalton Trans.*, (1981) 2147; R. S. Downing and F. L. Urback, *J. Am. Chem. Soc., 91* (1969) 5977; S. E. Harnung, B. S. Sorensen, I. Creaser, H. Maegaard, U. Pfenninger and C. E. Schaffer, *Inorg. Chem., 15* (1976) 2123; M. Ishimori, H. Aoi, T. Takeichi and T. Tsuruta, *Chem. Lett.*, (1976) 645.

11 R. D. Archer, R. O. Day and M. L. Illingsworth, *Inorg. Chem., 18* (1979) 2908.

12 H. A. Staab and F. Vogtle, *Chem. Ber., 98* (1965) 2691.

13 M. I. M. Wazer, *Ph.D. Thesis*, University of East Anglia, 1976. The program WAX is part of a library of computer programs described in a manual entitled *The NMR Program Library* by D. J. Loomes, R. K. Harris and P. Anstey, published in 1979 by the Science Research Council Daresbury Laboratory, Daresbury, Warrington, Cheshire, WA4 4AD, UK. Details may be obtained from W. Smith, Daresbury Laboratory.

14 M. G. B. Drew, *Coord. Chem. Rev., 24* (1977) 179.

15 J. L. Hoard and J. V. Silverton, *Inorg. Chem., 2* (1963) 235.

16 R. J. Clark, J. Lewis and R. S. Nyholm, *J. Chem. Soc.*, (1962) 2460.

17 R. D. Gilliom, *Introduction to Physical Organic Chemistry*, Addison-Wesley, Reading, MA, 1970, p. 121.

18 M. L. Illingsworth and R. D. Archer, *Polyhedron, 1* (1982) 487.

19 N. B. Pahor, M. Calligaris, P. Delise, G. Dodic, G. Nardin and L. Randaccio, *J. Chem. Soc., Dalton Trans.*, (1976) 2478.

20 M. Gulloti, L. Casella, A. Pasini and R. Ugo, *J. Chem. Soc., Dalton Trans.*, (1977) 339.

21 S. P. Dagnall, D. N. Hague and A. D. Moreton, *J. Chem. Soc., Dalton Trans.*, (1988) 1989.

22 F. Marumo, Y. Utsumi and Y. Saito, *Acta Crystallogr., Sect. B, 26* (1970) 1492.

23 G. Schwarzenbach and R. Baur, *Helv. Chim. Acta, 39* (1956) 722.

24 N. Bresciani, M. Calligaris, G. Nardin and L. Randaccio, *J. Chem. Soc., Dalton Trans.*, (1974) 1606.

25 C. J. L. Lock and P. Pilon, *Acta Crystallogr., Sect. B, 37* (1981) 45.

26 M. L. Illingsworth, L. J. Schwartz and B. P. Cleary, unpublished results.
27 (a) M. Goto, M. Takeshita and T. Sakai, *Inorg. Chem., 17* (1978) 314; (b) R. M. Silverstein and G. C. Bassler, *Spectrometric Identification of Organic Compounds*, Wiley, New York, 1967, p. 132.
28 C. G. Overberger and G. Montaudo, *J. Polym. Sci. C, 31* (1970) 33.
29 C. J. Hawkins, R. M. Peachey and C. L. Szoredi, *Aust. J. Chem., 31* (1978) 973.
30 M. F. Gargallo, J. D. Mather, E. N. Duesler and R. E. Tapscott, *Inorg. Chem., 22* (1983) 2888.
31 N. B. Pahor, M. Calligaris, P. Delise, G. Dodic, G. Nardin and L. Randaccio, *J. Chem. Soc., Dalton Trans.,* (1976) 2478.
32 M. L. Illingsworth, B. P. Cleary and A. J. Jensen, unpublished results.